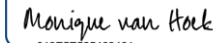


MAGNETIC NANOTRAP PARTICLES CAPTURE AND ENRICH BACILLUS ANTHRACIS ANALYTES IN BLOOD

by

Brittany Heath
A Thesis
Submitted to the
Graduate Faculty
of
George Mason University
in Partial Fulfillment of
The Requirements for the Degree
of
Master of Science
Biology

Committee:

DocuSigned by:

019E5E525463461...

Dr. Monique van Hoek, Thesis Chair

DocuSigned by:

1C0808F2310A4EC...

Dr. Kylee Kehn-Hall, Committee Member

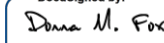
DocuSigned by:

47D4C917D2A94C1...

Dr. Barney Bishop, Committee Member

Digitally signed by Iosif Vaisman
DN: cn=Iosif Vaisman, o=George Mason University, ou=School of Systems Biology,
email=ivaisman@gmu.edu, c=US
Date: 2020.05.26 15:00:41 -04'00'

Dr. Iosif Vaisman, Director,
School of Systems Biology

DocuSigned by:

2D845FBC2DD8450...

Dr. Donna Fox, Associate Dean,
Office of Student Affairs & Special
Programs, College of Science



Dr. Ali Andalibi, Dean, College of
Science

Date: 05/29/2020

Summer Semester 2020
George Mason
University Fairfax, VA

Magnetic Nanotrap Particles Capture and Enrich Bacillus anthracis Analytes in Blood
A Thesis submitted in partial fulfillment of the requirements for the degree of Master of
Science at George Mason University

by

Brittany Heath
Bachelor of Science
Virginia Polytechnic Institute and State University, 2015
Bachelor of Science
Virginia Polytechnic Institute and State University, 2012

Director: Monique van Hoek, Professor
Department of Biology

Summer Semester 2020
George Mason University
Fairfax, VA

Copyright 2020 Brittany Heath
All Rights Reserved

DEDICATION

For my family, with their love and support all things are possible.

ACKNOWLEDGEMENTS

I would like to thank my thesis advisor, Dr. Monique van Hoek, for her mentorship and support throughout this process and the last three years. I will forever appreciate the opportunity to attend George Mason University in your lab and will miss you dearly.

I would like to thank Dr. Kylene Kehn-Hall for her role on my thesis committee and mentorship. I am excited to continue my education and research as a PhD student in your lab.

I would also like to thank Dr. Barney Bishop for his role on my thesis committee and the many laughs provided throughout my time here.

Many thanks go to Alex Ii for helping with *Bacillus* nanotrap work. A lot of time has been spent troubleshooting procedures and obtaining data, in which your help is greatly appreciated.

I would also like to thank Ceres Nanosciences for providing the nanotrap particles. Special thanks to DTRA for funding this project.

TABLE OF CONTENTS

	Page
List of Tables	vii
List of Figures	viii
List of Abbreviations and/or Symbols	ix
Abstract	x
Introduction	1
Results	5
Magnetic nanotraps bind and enrich <i>B. anthracis</i> bacteria	5
Nanotrap particles bind and enrich <i>B. anthracis</i> proteins	9
Nanotraps particles effect on <i>B. anthracis</i> nucleic acid	27
Discussion	32
Materials and Methods	36
Bacterial Strain, Human Whole Blood, and NT Particles	36
Bacterial Binding and Stability in Blood	36
Bacterial Enrichment	37
Comparison of Pelleting NTs to Centrifugation	37
Whole Cell Lysate	38
Preparation of NT-Bound Proteins for Proteomics Analysis	38
LC-MS/MS Proteomic Analysis	39
Analysis of Proteomic Data	40
Western Blots	40
DNA Extraction and qPCR	41
Nucleic Acid Binding and Stability	42
DNase Protection Assay	42
Bacteria to Nucleic Acid Experiment	43
Software and Statistical Analysis	43
References	44

LIST OF TABLES

Table	Page
Table 1. Top 20 proteins identified bound to nanotraps from <i>Bacillus anthracis</i> Sterne strain whole cell lysate.....	15
Table 2. Top 20 proteins identified bound to nanotraps from <i>Bacillus anthracis</i> Sterne strain whole bacteria.	16
Table 3. Proteins from whole cell lysate enriched by binding to nanotraps (>2.5-fold enrichment) ordered in decreasing enrichment value.	17
Table 4. Proteins from whole bacteria enriched by binding to nanotraps (>2.5-fold enrichment), ordered in decreasing enrichment value.	18

LIST OF FIGURES

Figure	Page
Figure 1. Magnetic nanotraps (CN3080) captured and enriched <i>B. anthracis</i>	6
Figure 2 Nanotraps effect on bacterial concentration from biological matrices in comparison to centrifugation.	8
Figure 3. Proteomic analysis of nanotrap-bound proteins.	10
Figure 4 Analysis of proteomic data, predicted protein subcellular localization.....	20
Figure 5. Protein-protein interactions for enriched “nanotrap-bound proteins from WCL”.	23
Figure 6. Protein-protein interactions for enriched “nanotrap-bound proteins from Bacteria”.	24
Figure 7. Protein-protein interactions depicting nodes that share a metabolic pathway. .	25
Figure 8. Protein-protein interactions depicting nodes that share a PFAM protein domain for S-layer proteins.	26
Figure 9. Magnetic nanotraps ability to bind to <i>B. anthracis</i> Sterne SodA1 protein.....	27
Figure 10. Nucleic acids bound to magnetic nanotraps under increasing temperatures and prolonged incubation.	28
Figure 11. DNase protection assay.	30
Figure 12. Nanotrap (CN3080) capture of nucleic acid from blood spiked with whole bacteria.....	31

LIST OF ABBREVIATIONS

<i>Bacillus anthracis</i>	<i>B. anthracis</i>
Brain Heart Infusion	BHI
Colony Forming Units	CFU
Dulbecco's Phosphate Buffer Saline	DPBS
False Discovery Rate	FDR
Luria Broth.....	LB
Nanotraps	NT
Normalized Value	NV
Peptide Spectrum Match	PSM
Poly(N-isopropylacrylamide)	NIPAm
Polyvinylidene fluoride.....	PVDF
Room Temperature	RT
Superoxide Dismutase A1.....	SodA-1
Tris-Buffered Saline with 0.1% Tween 20	TBS-T
Whole Cell Lysate.....	WCL

ABSTRACT

MAGNETIC NANOTRAP PARTICLES CAPTURE AND ENRICH BACILLUS ANTHRACIS ANALYTES IN BLOOD

Brittany Heath, M.S.

George Mason University, 2020

Thesis Director: Dr. Monique van Hoek

Bacillus anthracis is a Category A biological threat agent as it has the potential to be used as a bioweapon. It is also encountered in nature where it can persist in the environment for decades. Nanotraps are hydrogel microparticles that have been developed to bind a wide variety of bio-analytes. The use of nanotraps can potentially capture biomarkers such as proteins or nucleic acids, enabling analytes that were once below detectable limits to become detectable by various processes such as mass spectrometry. The purpose of this study was to characterize the ability of magnetic nanotrap particles to capture, enrich and stabilize *Bacillus anthracis* biomarkers and bacteria. We have shown that magnetic nanotraps, functionalized with a Reactive Red 120 affinity bait, are able to capture and enrich *Bacillus anthracis* bacteria and proteins. These nanotraps have also been demonstrated to bind to *Bacillus anthracis* nucleic acid and protect it from degradation when incubated with DNase. Magnetic nanotraps can also allow for rapid separation of

biomarkers from complex biological matrices, such as whole blood, performing just as well as centrifugation in this separation. Overall, this work suggests that nanotraps may be a useful part of up-stream processing and may improve detection in a workflow to detect *Bacillus anthracis* bacteria, proteins or nucleic acids from whole human blood.

INTRODUCTION

Bacillus (B.) anthracis is a gram-positive, rod-shaped, spore forming bacterium and the etiological agent for anthrax. This bacterium has multiple routes of infection, including cutaneous, gastrointestinal and inhalational (1). Due to the potential and historical use of *B. anthracis* as a biological weapon, this pathogen is considered a Tier 1 Select Agent (2). The primary concern of this bacterium is as a bioterror agent, given the anthrax attacks in 2001, but can also be encountered in nature. People may be exposed when interacting with animal skins or wool, deceased animals or working in the environment, specifically the soil (3).

The life cycle of *B. anthracis* alternates between vegetative bacteria and bacteria that has undergone sporulation. Vegetative cells that have been shed or released into the environment in the vegetative form are triggered to sporulate due to adverse conditions, as well as the presence of oxygen (4). These spores may remain dormant for decades before being taken up by a new host, in which the spores can then germinate and disseminate through a series of biological processes. The new host will continue this cycle by shedding bacteria into the environment ante- and post-mortem. This release allows the cells to sporulate and once again reenter the environment, waiting to be picked up by a new host. (5)

Time of intervention is paramount for anthrax infections due to the high mortality rate (95-100%) if not treated aggressively (6). The importance of early detection in effective treatment makes rapid diagnostics a high priority. The diagnostic gold standard for determining positive anthrax infections remains to be culturing the sample (6). However, culturing may result in a false-negative when there are low quantities of viable bacterial cells. PCR is becoming an accepted standard in detection for *B. anthracis* and specifically targeting genes that encode for toxins and the characteristic capsule (1, 7, 8). The genes located on plasmids pXO1 and pXO2 of fully virulent *B. anthracis* strains, encode for protective antigen, lethal factor, edema factor and poly-D-glutamic acid capsule (5, 6). While these diagnostics have proven to be successful, detection in complex biological matrices can prove challenging, as well as time sensitive transferring of samples to the lab. Currently, cold-chain transport is used as a mechanism to transfer suspect anthrax samples to the Center of Disease Control, or other approved laboratories, for confirmation in which time is of utmost important for diagnostic testing, especially for culturing bacteria (1). These limitations led us to explore alternative methods of sample separation from complex biological matrices and potential analyte stabilization to alleviate or ameliorate the need of cold-chain transport. Such improvements may improve detection and diagnosis of anthrax infections, which could be lifesaving.

Advancements in nanobiotechnology have proven beneficial for the forward progression in the development of diagnostic assays and easier or quicker overall processing of biological samples. A recently developed novel technology includes the use of nanotrap (NT) hydrogel microparticles to improve analyte detection and increase

overall ease of upstream processing of samples (9). Ceres Nanosciences offers multiple particle types that consist of a cross-linked poly(N-isopropylacrylamide) (NIPAm) core, functionalized with a variety of chemical affinity baits (most commonly industrial dyes) , in which several of these dyes have previously been used in affinity chromatography (9-11). These particles can then be further functionalized via the binding of ferromagnetic particles to the outside of the core allowing for easier separation without the need for centrifugation (10, 11). Ceres Nanosciences has provided us with core NTs, functionalized with Reactive Red 120 and ferromagnetic particles. Prior studies have shown NTs ability to concentrate low molecular weight proteins and other low abundance biomarkers (12, 13). In addition to concentrating biomarkers to a detectable limit, the particles have also been shown to preserve RNA and proteins at elevated temperatures and extended incubation times (13, 14). NTs have been shown to enhance detection of biomarkers for several infectious pathogens such as *Borrelia burgdorferi*, Venezuelan eastern equine encephalitis virus, Rift Valley fever virus, HIV, and Chagas disease (10, 13, 14). NTs also allow for easy separation from complex biological matrices such as blood, serum, urine, sweat, and nasal swabs (15, 16).

Our lab sought to characterize the ability of these NT particles to capture *B. anthracis* analytes in buffers and whole human blood as part of an effort to make a multi-pathogen detection system. The particle type CN3080, a magnetic particle functionalized with Reactive Red 120, was chosen for this project as it had previously been shown to be the optimal particle type for multi-viral and bacterial capture, as seen in its ability to enrich both VEEV and *Francisella* analytes (14). In addition to testing for the ability to

capture *B. anthracis* biomarkers and whole bacteria, we tested the ability of CN3080 to preserve these biological markers at elevated temperatures and increasing incubation times. This NT technology has the potential to improve workflow in streamlining the up- and down-stream processing and allows for easier separation of target analytes from complex biological matrices such as whole blood.

RESULTS

We sought to characterize the use of magnetic NTs as a way to improve detection of *B. anthracis* analytes, including proteins (i.e. SodA-1), nucleic acids (i.e. genes for protective antigen and PL3) and bacteria, as culturing still remains the gold standard in determining a positive anthrax case and bacteria may be needed for forensic investigation. (6, 17). Our overarching goal was to address the difficulties associated with sample preparation and storage, in addition to enriching analytes that fall below the detection limit. The ability to use NTs as a means of biomarker separation and stabilization from complex biological matrices could lead to quicker sample preparation and negate the need for cold-chain transport. Lastly, the ability to enrich analytes from biological matrices could improve detection of biomarkers that were once below the detection limit, decreasing false-negatives results . To assess the NTs ability to provide an improvement in detection of *B. anthracis*, our experimental design focused on the particles ability to capture, stabilize, and enrich *B. anthracis* Sterne strain for the different classes of biological markers.

Magnetic nanotraps bind and enrich *B. anthracis* bacteria

To determine if NTs would be able to assist in overcoming the aforementioned barriers associated with biological samples, we first tested the magnetic CN3080 NTs ability to capture and bind *B. anthracis* bacteria in human whole blood. After 30-minute

sample incubation with or without particles, the NT samples were pelleted, supernatant discarded and then the pellet resuspended in phosphate buffer saline (PBS). The samples were then serially diluted and plated. There was a significant difference observed in the number of *B. anthracis* bacteria (CFU/mL) detected between bacteria in blood and bacteria bound to NTs in blood, as seen in **Figure 1A**. Despite this difference, our results indicate that the CN3080 magnetic NTs, functionalized with Reactive Red 120, are able to bind *B. anthracis* bacteria in a complex biological matrix including human whole blood.

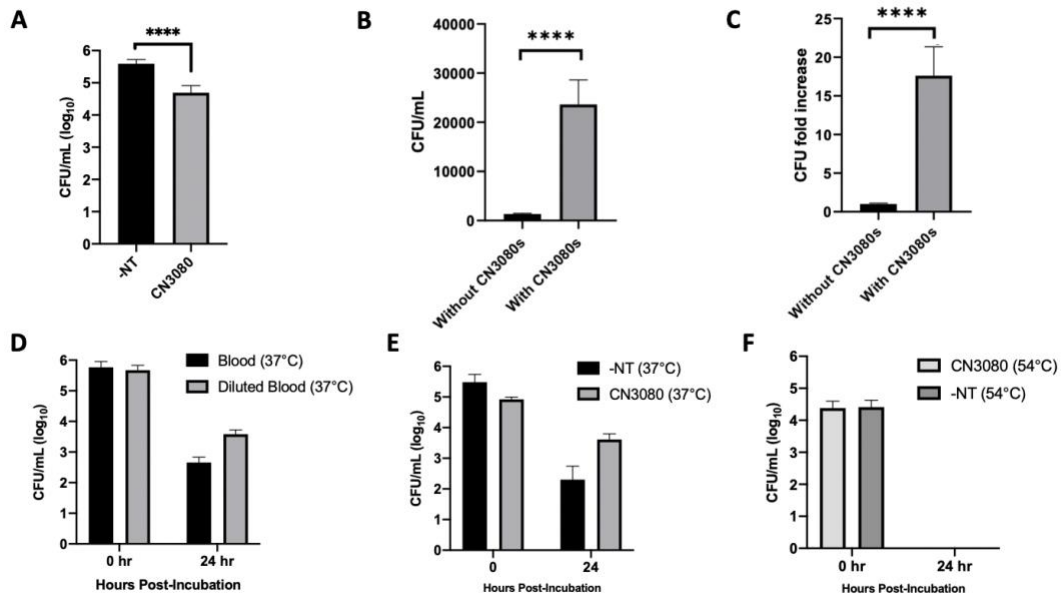


Figure 1. Magnetic nanotraps (CN3080) captured and enriched *B. anthracis*. *B. anthracis* Sterne strain was spiked and incubated, in the presence or absence of CN3080 NTs, in (A) human whole blood (RT, 30 min.) to assess particles' ability to capture bacteria. (B) 1mL PBS (RT, 2 h) to test for particle enrichment of whole bacteria, (C) same as (B), represented as fold increase. Bacterial stability was determined in whole blood vs. blood diluted 1:10 in PBS without particles (D) and with particles in human whole blood up to 24 h at 37°C (E) and 54°C (F).

Previous studies have shown the NTs ability to enrich detection of biological markers in complex biological matrices, such as the detection of low abundance markers in urine (15). To determine the enrichment properties of the magnetic CN3080 NTs with whole bacteria, we spiked a low starting concentration of *B. anthracis* Sterne strain into a larger volume of PBS or blood and incubated samples for two hours in the presence and absence of NTs. There was a significant difference seen in the number of bacteria captured by NTs (**Figure 1B**) with approximately a 15-fold increase (**Figure 1C**) when compared to that of bacteria in PBS alone. When testing bacterial enrichment in human whole blood (**Figure 2A**), there was the same significant increase in NT-bound bacterial capture as seen previously in PBS. In addition, a new particle type was introduced into the study. Previous particles were kept at 4°C in a storage buffer prior to use. The same magnetic core particles, functionalized with Reactive Red 120, were also provided to us in the lyophilized form to use in preliminary studies. These particles proved to enrich *B. anthracis* bacterial capture in blood better than the particles kept in storage buffer (**Figure 2A**). To further compare our methodology of incorporating NTs into up-stream sample processing, we compared the use of centrifugation to NT-assisted pelleting of *B. anthracis* bacteria (**Figure 2B**).

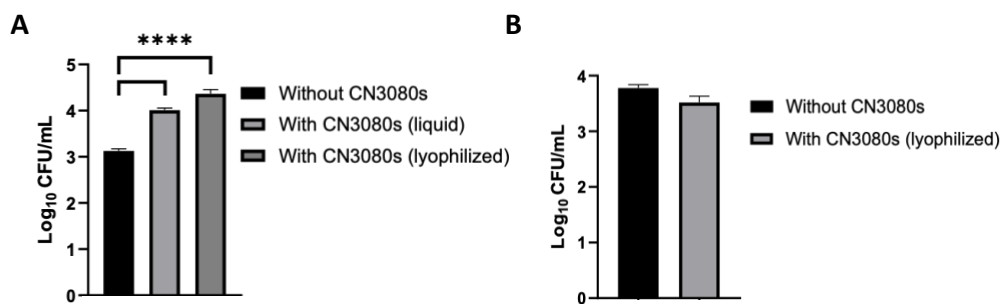


Figure 2 Nanotraps effect on bacterial concentration from biological matrices in comparison to centrifugation.

(A) 1mL of spiked DPBS (10³ CFU/mL) was incubated in the presence and absence of magnetic CN3080 NT particles for 2 h at RT. (B) 1mL of spiked human whole blood (10⁴ CFU/mL) was incubated in the presence and absence of magnetic NT particles for 2 h at RT. Samples were pelleted either by centrifuge (-NT) or magnetic rack (+NT), resuspended in DPBS and serial dilutions plated.

Our results indicate CN3080 NTs can enrich *B. anthracis* bacteria from biological matrices when present in low concentrations and particles can perform just as well as standard centrifugation. This equivalent performance of concentrating bacteria using NTs may circumvent the need for technical equipment, such as centrifuges, that may not be readily available.

Cold-chain transport is required for the movement of suspect human blood and serological samples (1). To address the issue of sample storage in adverse conditions, we next characterized the particle's ability to stabilize whole bacteria in blood at elevated temperatures. To determine the effects of blood on bacterial growth, we spiked blood and diluted blood (1:10) with *B. anthracis* Sterne strain and incubated samples at 37°C for 24 hours, followed by serial plating. Without the addition of particles, there was an initial decrease seen in bacterial growth in whole blood comparable to the diluted blood (**Figure**

1D). We next incorporated the use of the magnetic CN3080 NTs, incubating bacteria in undiluted blood at 37°C (**Figure 1E**) and 54°C (**Figure 1F**) up to 24 hours. Samples were processed the same as before. Our results indicated there was no difference seen in bacterial survival at 24 hours with the addition of NTs, with complete bacterial death when incubated at 54°C. We concluded that magnetic NTs are not able to stabilize bacteria when incubated in blood at elevated temperatures.

Nanotrap particles bind and enrich *B. anthracis* proteins

As previously mentioned, low abundance proteins such as human growth hormone have been enriched by nonmagnetic NT particles, functionalized with different chemical dyes, allowing for the detection of these proteins using mass spectrometry (15). It was hypothesized that the CN3080 magnetic NTs would bind and enrich *B. anthracis* proteins from whole cell lysate spiked into phosphate buffer saline (PBS). In addition, a comparison of mass spectrometry analysis was made between whole cell lysate (WCL) bound to NTs and whole bacteria bound to NTs. PBS was spiked with either WCL or bacteria and then incubated at room temperature for 30 minutes. The NT samples were then pelleted using the MagRack and the supernatant discarded. Both samples were submitted for mass spectrometry analysis as outlined in the methods and materials section. Proteomic analysis revealed 636 total proteins in WCL and 765 total proteins in NT-bound WCL, with 521 of those hits shared between the two groups (**Figure 3A**).

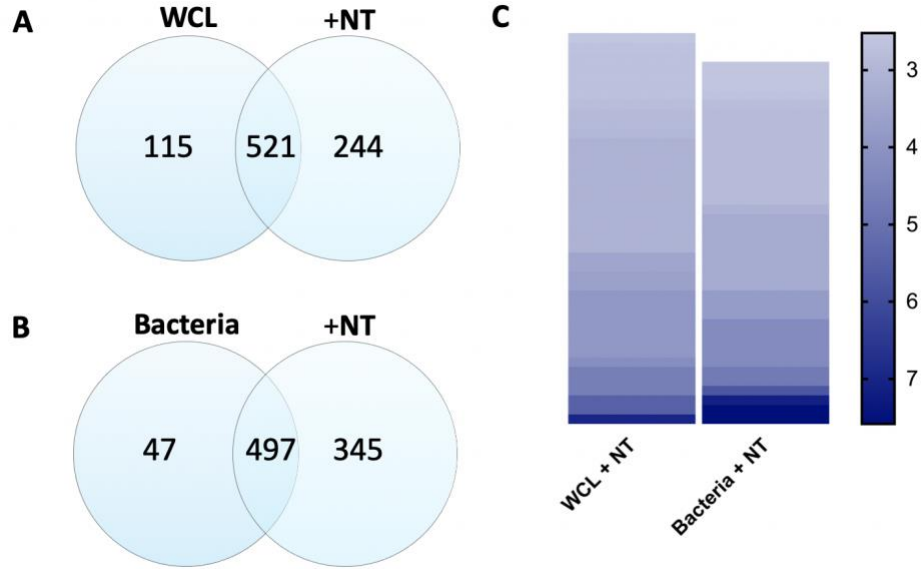


Figure 3. Proteomic analysis of nanotrap-bound proteins.

(A) Venn diagram depicts shared proteins and unique proteins for spiked whole cell lysate (WCL) in buffer compared to lysate incubated and bound to CN3080 NTs (+NT). (B) Venn diagram depicts shared proteins and unique proteins for spiked bacteria in buffer compared to bacteria bound to NT. (C) Abundance (PSMs) from proteomic analysis for both WCL and Bacteria were normalized and protein enrichment by binding to NTs is illustrated by the increasing color intensity as seen in the heat map (highest enrichment values = darkest blue). N=1

115 proteins were found to be unique to the WCL control sample and 244 unique proteins in NT-bound WCL. Mass spectrometry analysis of *B. anthracis* whole bacteria resulted in 544 total proteins in the control group and 842 proteins in the NT-bound sample (Figure 3B). 497 proteins were hits for both the control group and the NT-bound protein group, with 47 proteins unique to the control sample and 345 proteins unique to the NT-bound sample.

Peptide enrichment was quantified based on protein abundance, peptide spectrum matches (PSMs). First, shared and unique proteins were identified, numerical value of

zero for #PSMs was assigned to groups (control or NT-bound) in which they did not share a peptide hit so that they may be incorporated into the calculations. Given the difference in the total number of proteins between the control and experimental group, the values had to be normalized. Normalization was done by taking the #PSMs for an individual protein and dividing it by the total #PSMs in the sample.

$$\frac{\text{\#PSMs}}{\text{Total PSMs}} = \text{normalized value for individual protein (NV)}$$

This was done for both the control group and NT group. Next, enrichment values were calculated as follows:

$$\frac{\text{NV for NT bound protein}}{\text{NV for control protein}} = \text{Enrichment value}$$

Proteins were then sorted based on enrichment value, from largest to smallest with a >2.5 fold-enrichment cutoff (**Table 3, Table 4**).

Proteins with a numerical value greater than 2.5 were considered to have been enriched by NTs. A heat map was constructed of enriched proteins based on fold-enrichment values, depicting *B. anthracis* proteins enriched by NTs for both WCL and whole bacteria (**Figure 3C**). Values for fold-enrichment are represented by varying hues of blue, with proteins that scored the highest enrichment value visualized as the darkest blue. It was concluded that the magnetic NTs are able to enrich proteins.

Further analysis of the top 20 proteins bound to magnetic NTs for both WCL and Bacteria (**Table 1, Table 2**) revealed commonality between the groups, sharing eight out of the twenty proteins. Three genes worth noting are AW20_2693, AW20_2694 and AW20_3985 encoding for translation elongation factor Tu (EF-Tu), translation

elongation factor G (EF-G) and chaperone protein DnaK. The PATRIC database was used to identify specialty genes within the *B. anthracis* subsp. Sterne genome (Genome ID: 260799.41) with a focus on transporters, virulence factors, genes known to contribute to antibiotic resistance and drug targets (18) (<https://patricbrc.org>).

The genes which encode EF-Tu, EF-G and DnaK were flagged as specialty genes, with EF-Tu and EF-G as contributors to antibiotic resistance and DnaK labeled as a transporter. *B. anthracis* spore surface protein, EF-Tu, has been shown to play a role in evading the human complement immune system by binding plasminogen and through a series of proteolytic events escape phagocytosis by macrophages (19). In addition, EF-Tu has an important role in protein synthesis by catalyzing the dissociation of tRNA from the ribosome (20). EF-G also plays an essential role in protein synthesis as it is a catalyst for translocation of the tRNA within the ribosome (21). There is some evidence that has predicted EF-G to be involved in protein synthesis initiation during spore revival, upon exiting the dormancy state (22). Antibiotic resistance can be acquired to drugs targeting either EF-G or the binding site on the ribosome through a point mutation, thus allowing translation (20).

DnaK is involved in many cellular processes including protein folding, heat shock survival and protein translocation (23-25). Prior studies have shown that DnaK is involved in the secretion of virulence factors, which can impact pathogenesis (26). The results for top NT-bound proteins were as expected due to the presence of high abundance proteins, such as DnaK (27).

Out of the non-shared top proteins bound to NT, PATRIC flagged *rpoB* (AW20_2699) as a specialty gene with known antibiotic resistance. The *rpoB* gene encodes for the RNA polymerase (RNAP) β subunit, which acts as a primary catalyst for transcription and is a common target for antibiotics, such as rifampicin (28). Rifampicin acts by binding the β subunit and alters the rate of transcription (29). Resistance can be acquired through mutations of the β subunit, in which the mutation can occur throughout the *Bacillus* lifecycle with potential impact on cellular processes involved in growth, maturation, sporulation and germination (29, 30).

When comparing top WCL NT-bound proteins to WCL proteins that were enriched by NTs (**Table 1, Table 3**), there were zero shared proteins between the two groups. Several genes were flagged as specialty genes by PATRIC for the enriched group, including AW20_4472 (*ileS*) and AW20_4752 (*tkt*). The gene *ileS* encodes for isoleucyl-tRNA ligase/synthetase (IleRS) and was listed as a gene that contributes to antibiotic resistance. The role of IleRS is to ensure the correctly charged amino acid is added onto its corresponding tRNA, a process essential in mRNA translation (31). Cellular machinery exists to proofread and make modifications to the amino acid pre- and post-attachment to ensure accurate mRNA translation (32, 33). One study investigated the importance of this proof-reading mechanism in *Bacillus subtilis*, concluding this aspect of IleRS is necessary for efficient sporulation (33). The second specialty gene in the WCL NT-bound proteins, *tkt*, encodes for the protein transketolase and was predicted by PATRIC as a potential drug target. Transketolase is an enzyme involved in microbial carbohydrate metabolism, taking part in the Pentose-Phosphate Pathway (PPP) and

producing products that are able to enter the glycolysis pathway (34, 35). This protein has shown to be a potential drug target in other pathogenic microbes, such as *Mycobacterium tuberculosis*, due to the low degree of homology of this protein between bacterial species and humans (34). Transketolase has also been shown to be an immunogenic protein, and is one component of the *B. anthracis* vaccine, showing potential for further modified anthrax subunit vaccines (36).

Unlike the protein data comparison for WCL NT-bound and WCL enriched proteins, there was one protein in common between the samples spiked with whole bacteria (**Table 2, Table 4**) but was not identified as a specialty gene. AW20_1849 (BAS0842, Sterne reference genome), listed as *eag* for *B. anthracis* Ames strain, produces the S-layer protein EA1. The enriched group however had one protein that was unique and listed as a specialty gene. This specialty gene, AW20_3846 (BA_4648 in *B. anthracis* Ames strain, *mreB*) was identified as a transporter. The protein *mreB* is a cell shape determining protein that has an important role in bacterial cytoskeleton development (37). In addition to maintaining the rod-shape of *B. subtilis*, the protein also plays a potential role in membrane diffusion (38, 39). These results support the validity of the assay since these genes are important to *B. anthracis* survival and pathogenesis.

Table 1. Top 20 proteins identified bound to nanotraps from *Bacillus anthracis* Sterne strain whole cell lysate.

Top whole cell lysate proteins bound to magnetic nanotrap particles

Locus Tag	Function	#PSMs
AW20_2511	chaperonin GroL	225
AW20_1849	hypothetical protein	96
AW20_2198	hypothetical protein	88
AW20_2693	translation elongation factor Tu	67
AW20_2719	negative regulator of genetic competence ClpC/MecB	57
AW20_4876	aldehyde dehydrogenase family protein	52
AW20_3175	phosphopyruvate hydratase	49
AW20_1255	stage IV sporulation protein A	45
AW20_2694	translation elongation factor G	42
AW20_2512	10 kDa chaperonin	41
AW20_3003	ATP synthase F1, beta subunit	39
AW20_4815	aconitate hydratase 1	37
AW20_463	methyalmalonate-semialdehyde dehydrogenase	37
AW20_544	zinc-binding dehydrogenase family protein	36
AW20_2460	putative delta-1-pyrroline-5-carboxylate dehydrogenase	36
AW20_4541	translation elongation factor Ts	35
AW20_3985	chaperone protein DnaK	32
AW20_2090	bacterial extracellular solute-binding s, 5 Middle family protein	31
AW20_2422	peroxiredoxin	31
AW20_4445	transcription factor, RsfA family protein	31

Table 2. Top 20 proteins identified bound to nanotraps from *Bacillus anthracis* Sterne strain whole bacteria.

Top proteins from whole bacteria bound to magnetic nanotraps

Locus Tag	Function	#PSMs
AW20_2258	formate acetyltransferase	183
AW20_3175	phosphopyruvate hydratase	94
AW20_1850	S-layer protein sap	88
AW20_3928	aldehyde dehydrogenase family protein	86
AW20_2693	translation elongation factor Tu	80
AW20_2511	chaperonin GroL	78
AW20_2694	translation elongation factor G	78
AW20_3985	chaperone protein DnaK	77
AW20_544	zinc-binding dehydrogenase family protein	61
AW20_3173	triose-phosphate isomerase	57
AW20_1849	hypothetical protein	53
AW20_3171	glyceraldehyde-3-phosphate dehydrogenase, type I	52
AW20_4327	dihydrolipoyl dehydrogenase	51
AW20_3667	alanine dehydrogenase	48
AW20_3695	pyruvate kinase	48
AW20_2071	zinc-binding dehydrogenase family protein	47
AW20_4325	pyruvate dehydrogenase E1 component subunit beta	43
AW20_1266	hypothetical protein	43
AW20_2699	DNA-directed RNA polymerase, beta subunit	43
AW20_4541	translation elongation factor Ts	43

Table 3. Proteins from whole cell lysate enriched by binding to nanotraps (>2.5-fold enrichment) ordered in decreasing enrichment value.

Whole cell lysate proteins enriched by magnetic nanotraps

Locus Tag	Function	#PSM		Enrichment Value
		-NT	+NT	
AW20_1724	glycerol kinase	1	9	6.97
AW20_1455	polyhydroxyalkanoic acid synthase, PhaR subunit	1	7	5.42
AW20_2543	hypothetical protein	2	14	5.42
AW20_4580	insulinase family protein	1	6	4.65
AW20_135	hypothetical protein	1	6	4.65
AW20_679	nitrate reductase, beta subunit	1	6	4.65
AW20_2966	3-hydroxyacyl-CoA dehydrogenase, NAD binding domain protein	5	27	4.18
AW20_4472	isoleucine--tRNA ligase	1	5	3.87
AW20_2666	30S ribosomal protein S13	1	5	3.87
AW20_680	nitrate reductase, alpha subunit	1	5	3.87
AW20_3734	asparagine--tRNA ligase	1	5	3.87
AW20_1427	oligopeptidase	1	5	3.87
AW20_877	L-lactate dehydrogenase	1	5	3.87
AW20_4752	transketolase	3	15	3.87
AW20_1567	oligoendopeptidase F	3	14	3.61
AW20_3437	naphthoate synthase	3	14	3.61
AW20_3841	valine--tRNA ligase	2	9	3.48
AW20_3159	ATP-dependent Clp endopeptidase, proteolytic subunit ClpP	2	9	3.48
AW20_274	AMP-binding enzyme family protein	1	4	3.10
AW20_805	NH(3)-dependent NAD(+) synthetase	1	4	3.10
AW20_1457	polyhydroxyalkanoic acid inclusion protein PhaP	1	4	3.10
AW20_2745	S1 RNA binding domain protein	1	4	3.10
AW20_3699	citrate synthase 2	2	8	3.10
AW20_3174	phosphoglycerate mutase	1	4	3.10
AW20_3227	hypothetical protein	1	4	3.10
AW20_2398	bacterial extracellular solute-binding s, 3 family protein	2	8	3.10
AW20_2238	hypothetical protein	2	8	3.10
AW20_4511	DAK2 domain fusion YloV family protein	1	4	3.10
AW20_2364	terD domain protein	2	8	3.10
AW20_4594	acceptor oxidoreductase, beta subunit, pyruvate/2-ketoisovalerate family protein	1	4	3.10
AW20_2107	bacterial extracellular solute-binding s, 3 family protein	5	19	2.94
AW20_2258	formate acetyltransferase	4	15	2.90
AW20_467	2-methylcitrate dehydratase	7	26	2.88
AW20_2630	glutamine-fructose-6-phosphate transaminase	5	18	2.79
AW20_5404	ABC transporter family protein	2	7	2.71
AW20_763	bacterial extracellular solute-binding s, 5 Middle family protein	4	14	2.71

Table 4. Proteins from whole bacteria enriched by binding to nanotraps (>2.5-fold enrichment), ordered in decreasing enrichment value.

Proteins enriched from bacteria bound to magnetic nanotraps

Locus Tag	Function	#PSM		Enrichment Value
		-NT	+NT	
AW20_2115	alpha,alpha-phosphotrehalase	1	16	7.58
AW20_850	nitroreductase family protein	1	16	7.58
AW20_1610	ornithine--oxo-acid transaminase	1	15	7.11
AW20_561	asparagine synthase	1	12	5.68
AW20_1412	ribonucleotide reductase, all-alpha domain protein	1	10	4.74
AW20_2128	pyridoxal phosphate-dependent acyltransferase family protein	1	10	4.74
AW20_3224	hypothetical protein	1	9	4.26
AW20_680	nitrate reductase, alpha subunit	1	9	4.26
AW20_3706	DNA polymerase I	1	9	4.26
AW20_1738	OB-fold nucleic acid binding domain protein	1	9	4.26
AW20_3846	cell shape determining, MreB/Mrl family protein	1	9	4.26
AW20_3595	peptidase M20/M25/M40 family protein	1	8	3.79
AW20_1665	lipoyltransferase and lipoate-ligase family protein	1	8	3.79
AW20_2464	ATP-dependent DNA helicase PcrA	1	8	3.79
AW20_2634	arginase	1	7	3.32
AW20_5422	aminotransferase class-III family protein	2	14	3.32
AW20_2361	toxic anion resistance family protein	1	7	3.32
AW20_3222	tyrosine--tRNA ligase	2	14	3.32
AW20_3924	methyltransferase domain protein	1	7	3.32
AW20_3322	lipoyl synthase	2	14	3.32
AW20_4548	proline--tRNA ligase	1	7	3.32
AW20_4409	putative nucleotide-binding containing TIR-like domain protein	1	7	3.32
AW20_1839	N-acetylmuramoyl-L-alanine amidase family protein	2	13	3.08
AW20_3721	putative aminopeptidase ysdC	1	6	2.84
AW20_670	molybdenum cofactor synthesis domain protein	1	6	2.84
AW20_2150	nicotinate phosphoribosyltransferase family protein	1	6	2.84
AW20_1507	dihydrolipoyllysine-residue succinyltransferase, E2 component of oxoglutarate dehydrogenase complex	1	6	2.84
AW20_3430	mitochondrial biogenesis AIM24 family protein	1	6	2.84
AW20_4132	butyrate kinase	1	6	2.84
AW20_742	CBS domain protein	1	6	2.84
AW20_2711	cysteine--tRNA ligase	1	6	2.84
AW20_905	pyrimidine-nucleoside phosphorylase	1	6	2.84
AW20_2919	hypothetical protein	3	18	2.84
AW20_1849	hypothetical protein	9	53	2.79
AW20_4551	transcription termination factor NusA	2	11	2.61
AW20_4891	cold shock protein CspD	3	16	2.53

Additional analysis of the mass spectrometry data was conducted using PSORTb to predict protein subcellular localization (**Figure 4**). Protein localizations were

categorized as cell wall, cytoplasmic, cytoplasmic membrane, extracellular or unknown. Prediction results for mass spectrometry samples prepared from WCL were comparable between the NT-bound proteins and the control group, with the majority of proteins identified as cytoplasmic and the least amount of proteins classified as extracellular (**Figure 4A, 4B**). Similar to results for WCL, subcellular-localization prediction for NT-bound proteins prepared from Bacteria were comparable to the control group (**Figure 4C, 4D**). Comparing the results, for the NT-bound proteins from WCL to “NT-bound proteins from Bacteria”, revealed a higher percentage of proteins from WCL localized to the cytoplasmic membrane, unknown, and a slight increase in cell wall and extracellular proteins; whereas “NT-bound proteins from Bacteria” had a higher percentage of proteins predicted to be localized in the cytoplasm.

From the subcellular localization prediction, several proteins of interest were those categorized as extracellular. *B. anthracis* superoxide dismutase proteins (AW20_4023, AW20_2859) were predicted to be extracellular and present in both WCL and bacteria NT-bound mass spectrometry peptide hits. These proteins are important for infections, when the spore is phagocytosed by the macrophage and enters a superoxide anion environment it triggers the spore to germinate. The phagolysosome environment is normally detrimental to bacterial survival; however, *B. anthracis* have a group of proteins that is able to overcome these adverse conditions. Two of these proteins that aid in survival and pathogenesis include two superoxidase dismutase, SodA1 and SodA2. The presence of superoxide anions is what can ultimately lead to cell death. *B. anthracis* has developed mechanisms involving these proteins to counter this issue either by acquiring

iron or presenting manganese, which will bind to the oxygen radicals and create hydrogen peroxide and molecular oxygen. This allows for the continuation of *B. anthracis* germination and replication prior to cell lysis, toxin release and eventual septicemia. (40-42). It is not known if these proteins (SodA1, SodA2) are surface-associated or truly secreted. Other well-characterized and secreted proteins including the anthrax toxin proteins were not identified on the NTs.

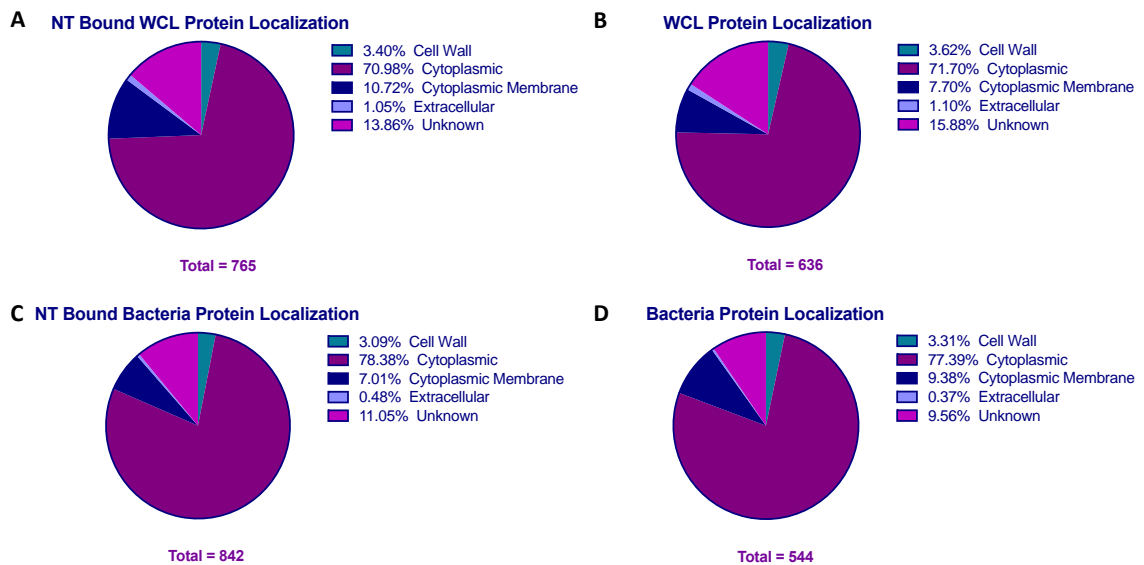


Figure 4 Analysis of proteomic data, predicted protein subcellular localization. Protein sequences obtained from mass spectrometry were submitted to PSORTb for subcellular localization prediction in (A) WCL bound to NTs (B) WCL control (C) whole bacteria bound to NT and (D) whole bacteria control.

Proteins from WCL and bacteria and enriched by NTs were evaluated for protein-protein interactions using STRING (Figure 5, Figure 6) to see if there were any important interactions between the NT-associated proteins. STRING analysis is a

database that has designed an algorithm to widely encompass varying datasets which support protein-protein interactions. These interactions vary from direct protein associations (i.e. co-expressed proteins) to indirect protein interactions (i.e. proteins that share a metabolic pathway). By incorporating these varying levels of support, from experimental evidence to computational prediction, STRING is able to bioinformatically predict both direct and indirect protein-protein interactions. (43).

Proteins labeled in STRING as narZ and clpP2 were found to be enriched by NTs for WCL and Bacteria. *B. anthracis* NarG (annotated as NarZ in STRING) is a nitrate reductase (44). *B. anthracis* nitrate reductase is able to reduce nitrite to nitrate and go through a series of biochemical processes to produce nitric oxide by a nitric oxide synthetase (NOS) (45, 46). The production of nitric oxide by *B. anthracis* plays a role in pathogenesis and virulence by protecting the germinating spore from the oxidative stress encountered within macrophages (47). The gene which encodes for ClpP2 is labeled as *clpP* in *B. anthracis* Sterne strain (AW20_3159, BAS5000 for reference strain) and *clpP2* in *B. anthracis* Ames strain (BA_5380). ClpP2 is a proteolytic subunit for the ATP-dependent Clp protease (48). The ClpP protein will bind another protein, ClpX, and the ClpXP protease has been shown in *Bacillus* spp. to have an important role in sporulation, germination, motility and growth under stress conditions (48-51).

Protein-protein interactions were further categorized for those NT-associated proteins identified in WCL, by the Kegg Pathway of “Microbial metabolism in diverse environments” (**Figure 7**). Three proteins enriched from Bacteria are shown to share the PFAM S-layer homology domain (eag, BAS0851, BAS1682) (**Figure 8**). The three locus

tags are AW20_1849, AW20_1839, AW_980 (annotated as eag, BAS0851 and BAS1682 respectively in STRING) encode for extractable antigen 1 (EA1) and two N-acetylmuramyl L-alanine amidase, family 3. S-layer proteins form a porous meshwork, an outer layer around *B. anthracis* to allow for selective permeability into and out of the cell. The S-layer is made up of several proteins (i.e. Sap and EA1), and differential gene expression is dependent on the varying environmental conditions (i.e. CO₂). S-layer proteins not only contribute to membrane permeability but also contribute to pathogenesis. These proteins have also been shown to elicit an immune response in guinea pigs and/or rabbits, indicating their potential use in future vaccine development (52, 53).

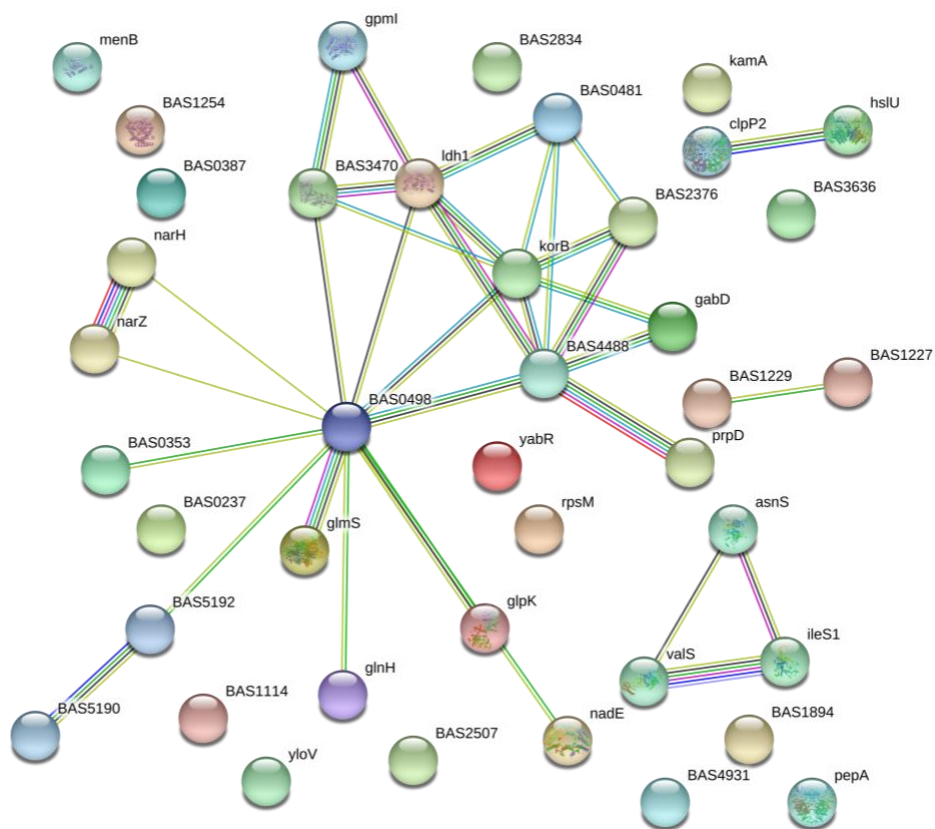


Figure 5. Protein-protein interactions for enriched “nanotrap-bound proteins from WCL”.

Proteins enriched (>2.5-fold enrichment) were analyzed using STRING for protein-protein interactions in proteins from WCL bound to NTs.

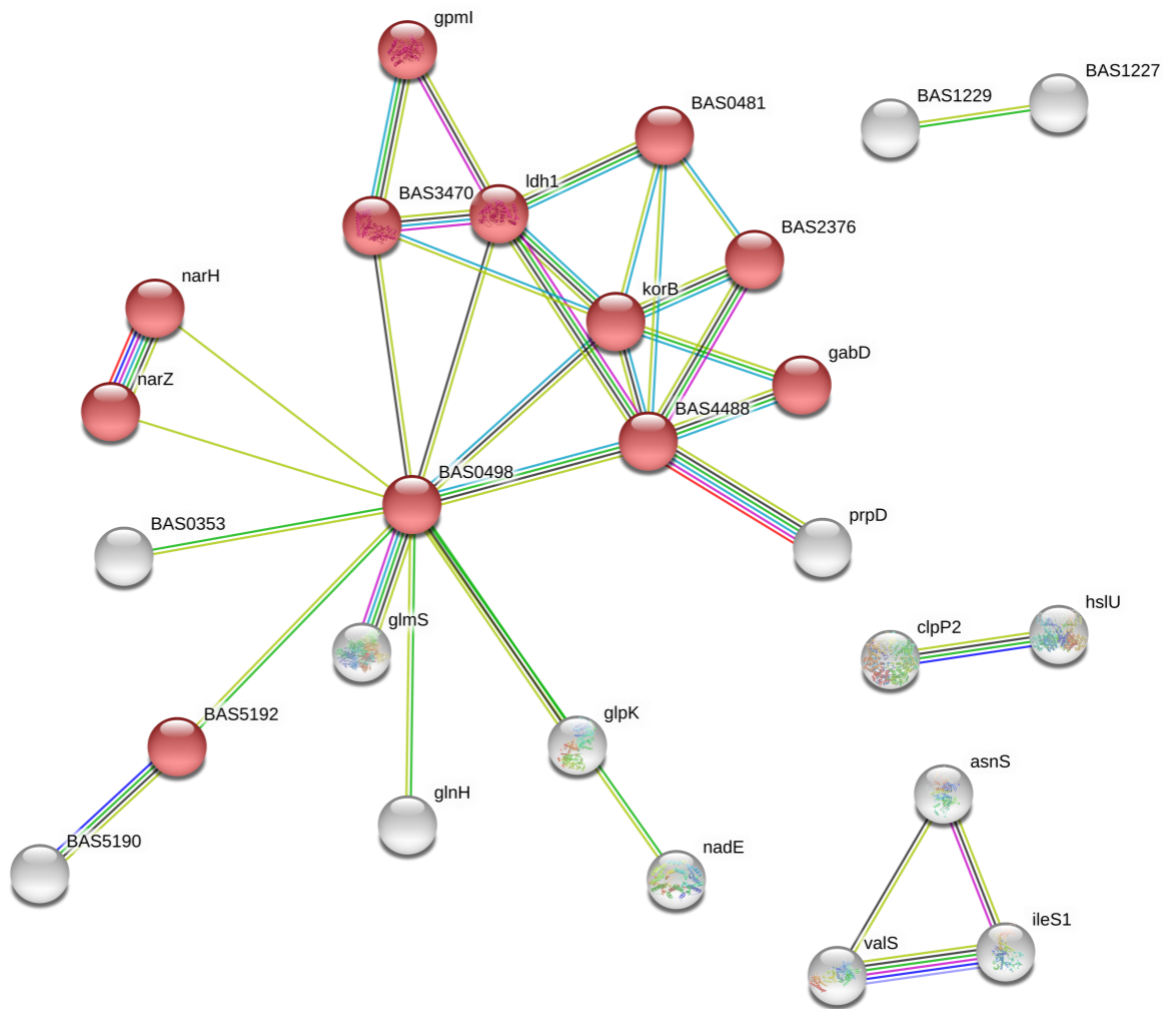


Figure 7. Protein-protein interactions depicting nodes that share a metabolic pathway.

Nodal connections (in red) of CN3080 NT-bound proteins enriched from WCL share a common KEGG Pathway involved in “microbial metabolism in diverse environments” (bat01120).

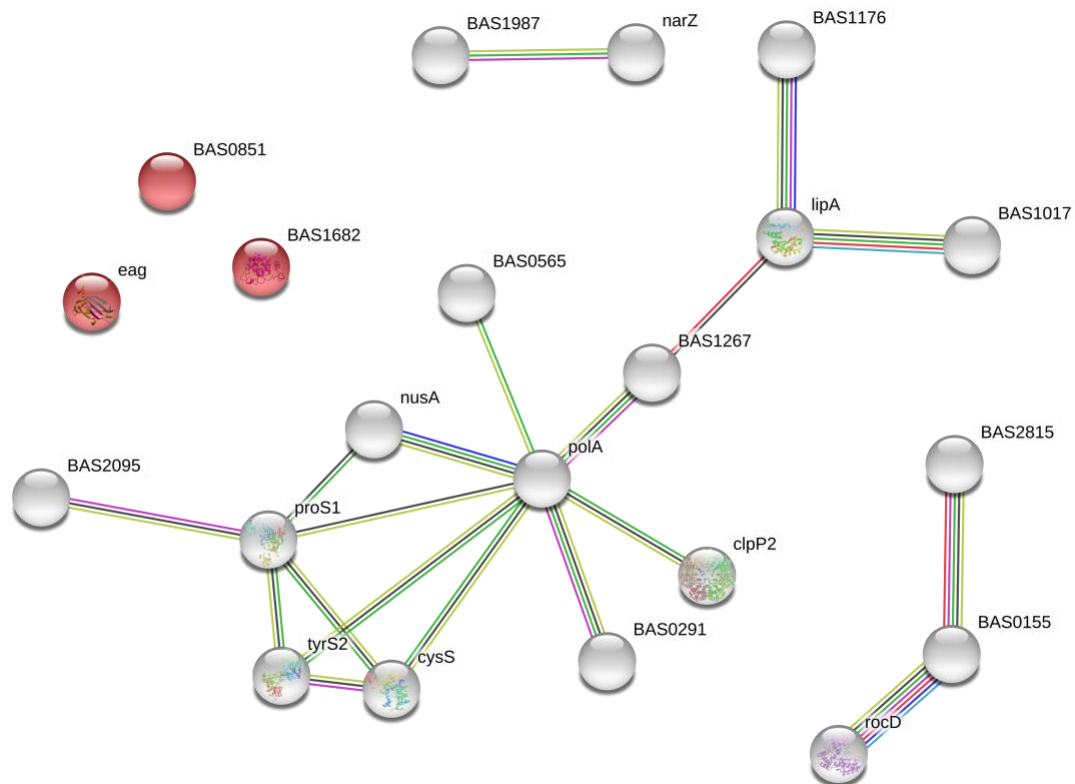


Figure 8. Protein-protein interactions depicting nodes that share a PFAM protein domain for S-layer proteins.

Nodes (in red) of CN3080 “NT-bound proteins enriched from Bacteria” share the S-layer homology domain (PF00395).

Based on proteins identified in the mass spectrometry analysis and antibodies available, western blotting was orthogonally conducted as an additional determinant of the NTs ability to bind proteins. *B. anthracis* SodA1 protein was identified in both WCL and Bacteria on mass spectrometry. WCL that was submitted for mass spectrometry analysis was also used for western blotting, with increasing concentration of NTs. Western blot analysis revealed the presence of SodA1 protein in both the control sample and NT-bound sample (**Figure 9A**). Since whole blood is the biologically relevant

matrix, western blotting was attempted using WCL spiked in undiluted and diluted whole blood (**Figure 9B**). Results for spiked blood were unable to be interpreted. Based on mass spectrometry and western blot analysis in buffer, it was concluded that the magnetic NTs are able to bind *B. anthracis* proteins.

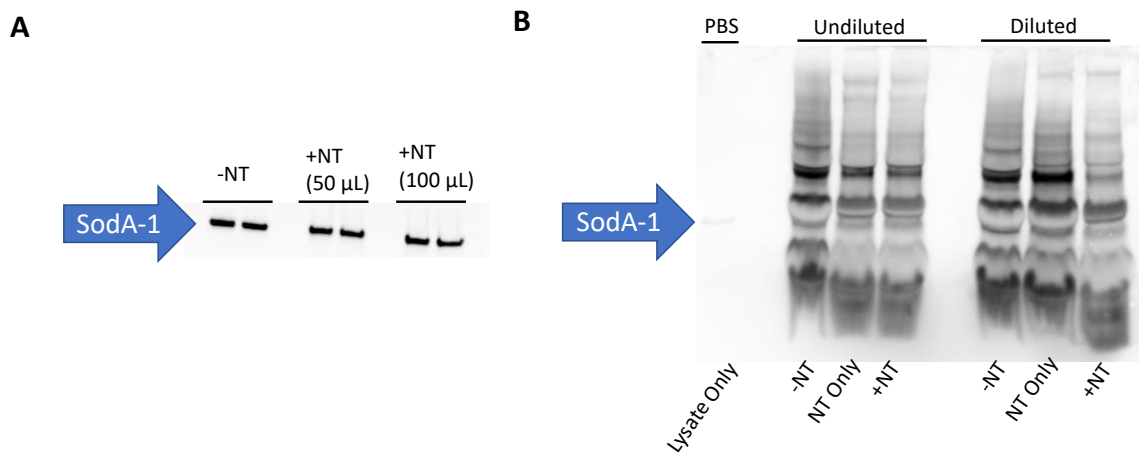


Figure 9. Magnetic nanotraps ability to bind to *B. anthracis* Sterne Soda1 protein. **(A)** Western blot analysis of whole cell lysate control (-NT) and bound lysate to CN3080 NTs (+NT) in DPBS at increasing NT concentrations. SodA-1 protein depicted by the blue arrow is approximately 23 kDa. **(B)** Western blot analysis of whole cell lysate in undiluted and diluted human whole blood with spiked PBS as the control.

Nanotraps particles effect on *B. anthracis* nucleic acid binding.

Our next set of experiments sought to characterize the NTs ability to bind and stabilize *B. anthracis* nucleic acid. To assess binding, human whole blood was spiked with purified nucleic acid and incubated in the presence or absence of NTs. After incubation, DNA was purified and qPCR performed to quantitate the amount of genomic copy number present in the samples, targeting the PL3 gene and *pag* gene. As it is

imperative to have a test with high specificity and accuracy, genes PL3 and *pag* were chosen as the biomarkers for detection of *B. anthracis* Sterne strain (pXO1+, pXO2-). PL3 (BA_5358, BAS4966) is a chromosomal marker specific to *Bacillus anthracis* strains and is found within the prophage lambdaBa03 region (54, 55). This chromosomal marker specific to *B. anthracis* was chosen due to the high degree of homology to other *Bacillus* spp., such as *B. cereus* (56). The *pag* gene, which encodes for protective antigen, was also chosen due to the presence of the pXO1 plasmid in the *B. anthracis* Sterne strain (57). If we were to test the fully virulent *B. anthracis* Ames strain (pXO1+, pXO2+) we would also target one of the *cap* genes encoded on the pXO2 plasmid (58).

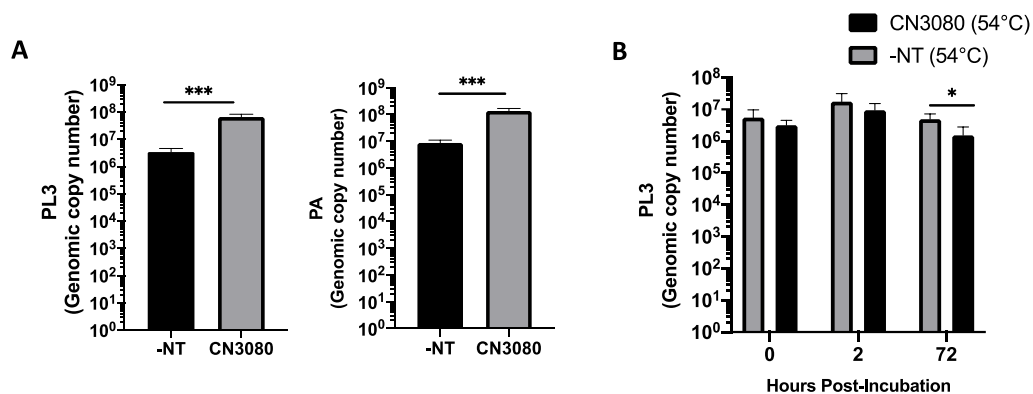


Figure 10. Nucleic acids bound to magnetic nanotraps under increasing temperatures and prolonged incubation.

(A) Purified nucleic acid was spiked into human whole blood and incubated (RT, 30 min.) to test binding to CN3080 NTs. NT samples were placed on a magnetic rack and washed once with PBS and resuspended in equal volume of PBS, prior to sample purification and qPCR. Target genes for qPCR was PL3 and PA. (B) NTs ability to stabilize nucleic acid was tested using purified nucleic acid incubated in blood (54°C, up to 72 h). Entire samples, including NTs (no wash step) were purified at designated time-points and quantified by qPCR.

A representative figure is shown (**Figure 10A**), depicting a significant increase in capture of *B. anthracis* nucleic acid from the biological matrix. Biological replicates varied in level of significance but an increase in capture was consistent. It was concluded that the magnetic NT particles can bind to *B. anthracis* nucleic acids. Our next step was to test the ability of CN3080 NT to stabilize preservation of nucleic acid. Human whole blood was spiked with purified nucleic acid and incubated at elevated temperatures (54°C) for extended period of time (72 hours). The number of genomic copies for PL3 were quantified. Differences were not observed between the NT and control samples at timepoints 0- and 2-hours post-incubation (**Figure 10B**). There was a significance seen between the control group and NT group after 72-hours incubation, with the control group having greater number of genomic copies than the NT samples. *B. anthracis* nucleic acid is already consistently stable across time, even at elevated temperatures (54°C). Further stabilization cannot be determined based on this study.

To find an alternate way of testing the NTs ability to stabilize *B. anthracis* nucleic acid, our next experiment was designed to test the NTs ability to protect purified nucleic acid from degradation in the presence of DNase. There was not a difference observed for the input values, as determined by samples not challenged with DNase (**Figure 11**). In comparing the NTs and control samples with DNase added, there was a significant difference between the two groups, with the NT-bound nucleic acid having an increase in recovered genomic copy number for both PL3 and PA. It was concluded the magnetic NTs have the potential to protect *B. anthracis* nucleic acid from degradation. Repeat experiments need to be conducted for a more concrete conclusion.

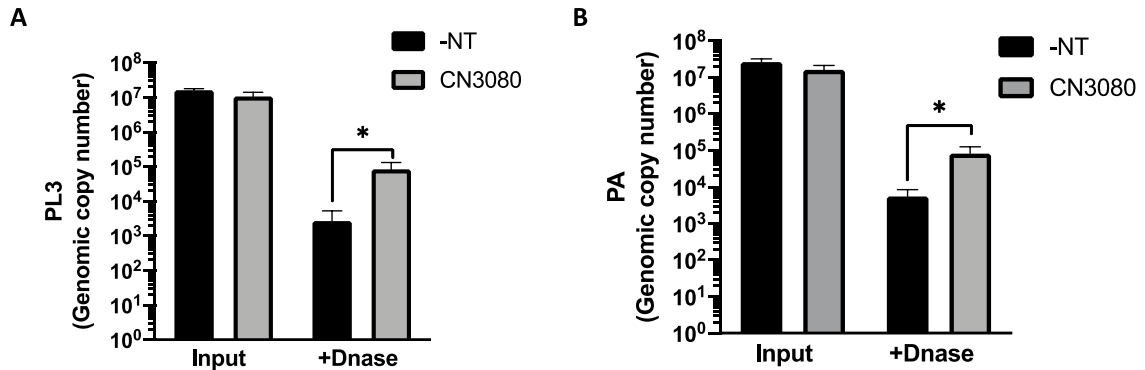


Figure 11. DNase protection assay.

Purified nucleic acid was spiked into human whole blood and incubated in the presence or absence of CN3080 NTs (RT, 30 min). After initial incubation, experimental samples were challenged and incubated with DNase overnight. Genomic copies were quantified by qPCR. The input value, spiked blood with and without NTs, were not statistically different. Significance was observed between control group and NT group when challenged with DNase. N=2, experiment performed one time.

Prior experiments depicted in this work showed complete bacterial death at 24 hours when *Bacilli* were incubated in blood at 54°C, suggesting that they may release their nucleic acid in this process. This last experiment was designed to quantify nucleic acids bound to CN3080 NTs in human whole blood spiked with *B. anthracis* bacteria. This study will allow us to characterize the ability of the NTs to bind and detect nucleic acid released due to the rapid bacterial die-off at 54°C.

The samples were once again incubated at elevated temperatures (54°C) for a prolonged incubation (72 hours). Samples were then processed for purified nucleic acid and quantified via qPCR. A difference in capture of nucleic acid was observed at timepoint 0- and 1-hour post-incubation for both the PL3 and *pag* gene (**Figure 9**).

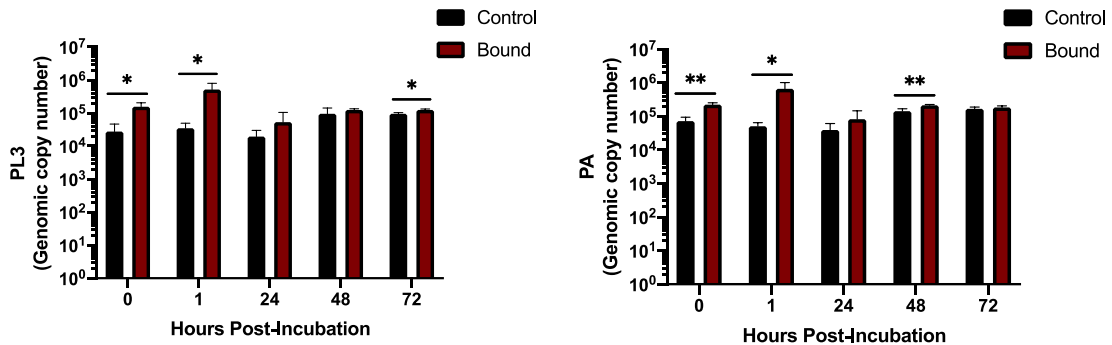


Figure 12. Nanotrap (CN3080) capture of nucleic acid from blood spiked with whole bacteria.

Bacteria was spiked into human whole blood and incubated (54°C, up to 72) for the indicated times. Nucleic acid was purified and quantified for both target genes, PL3 and PA. N=2, experiment performed one time.

Statistical analysis revealed significant differences between the control group and nucleic acid bound to NTs at 72 hours post-incubation for PL3 (**Figure 12A**) and 48 hours post-incubated for PA (**Figure 12B**). These data can be correlated with the bacteria survival results shown in **Figure 1F**, indicating that the bacteria quickly die off at 54°C, likely releasing their nucleic acids. Future studies should be conducted to confirm if bacterial death has an impact on nucleic acid capture. It was concluded that the magnetic CN3080 NTs can bind *B. anthracis* nucleic acid, in a complex biological matrix without negative impact, at elevated temperatures (54°C) and over time (72 hours).

DISCUSSION

Nanotrap (NT) particles have been shown to help enhance the limit of detection for analytes that correspond to biological markers or indicators of an infectious disease (14). It can be difficult to detect low abundance proteins in a complex biological matrix due to the presence of high abundance proteins (i.e. albumin) (11). The ability to increase detection is useful in research and development, such as for developing a novel assay or building upon an already existing technique. In addition, this ability to detect what was once undetectable can help improve testing and diagnostic accuracy, leading to a potential decrease in false negatives. Limit of detection is one facet scientists and laboratory personnel face when working with complex biological matrices such as blood, serum and/or urine.

Working with complex biological matrices comes with its own set of challenges, proving at times difficult in up-stream processing. Viability of samples become a concern when cold-chain transport may not be readily available or transport of samples may occur in adverse storage conditions (i.e. elevated temperatures, increased humidity, pro-longed storage times). Complexities may arise even once samples arrive to the designated personnel, for example blood may need to be further processed to separate red blood cells from serum. Geographical limitations can lead itself to shortages of necessary laboratory equipment such as centrifuges to processes patient samples. The use of NT particles may

help to fill that void or limitation that may be encountered with transport of patient samples and sample processing. With previous studies having shown the ability of these hydrogel microparticles to enhance limit of detection by enriching biomarkers and stabilizing analytes such as nucleic acids and proteins of various biothreat agents, our lab sought to apply these same particles and characterize their ability to bind, enrich and stabilize *B. anthracis* biological markers.

Our findings suggest that the CN3080 NT particles are able to bind *B. anthracis* bacteria in blood and enrich bacteria in PBS. Centrifugation and the use of magnetized NTs were also compared as a way of providing an alternative in cases where equipment, such as centrifuges, may not be available. Our results showed that the use of CN3080 magnetized NTs to capture bacteria in blood was comparable to centrifugation in efficiency. However, the particles did not stabilize bacterial survival in blood. We next characterized the magnetic CN3080 NT particles for their ability in binding and enrichment of bacillus proteins for. Protein binding and enrichment of several NT-bound *B. anthracis* proteins was observed when submitted for mass spectrometry analysis, as has been shown for VEEV viral proteins (14).

The ability to characterize stability of nucleic acid using CN3080 NTs proved to be initially difficult as *B. anthracis* nucleic acid was shown to already be stable, even in the presence of elevated temperatures. This led us to design an experiment to test whether or not CN3080 NTs can protect DNA from degradation by applying DNase to samples incubated with and without NT particles. QPCR results indicate an increased level in genomic copies were detectable in samples that were incubated with the NTs. These

preliminary experiments indicated that the CN3080 nanoparticles may have the potential to protect *B. anthracis* nucleic acid from degradation when challenged with nucleases.

The CN3080 NTs used in this paper were provided in a storage buffer suspension. It is possible that variability between experimental replicates could be due to having to aliquot the magnetic particles into different tubes with particles being retained on the pipette tip or tube sides. Ceres Nanosciences has developed an alternative to using wet particles through the production of lyophilized particles in a pellet, which we explored with some preliminary data in this paper. Their production team have created these particles in a ready-to-use pellet format already placed in a microcentrifuge tube which could decrease the variability between replicates. In addition, the magnetic core particles used in this paper (CN3080) did not stabilize *B. anthracis* bacteria or protein against degradation by high temperature or other factors. The CN3080 particles used in this paper were functionalized with Reactive Red 120 affinity bait. Ceres Nanosciences offers many other types of particles with different affinity baits. While we chose to use the particle type CN3080 for its multi-pathogen capture abilities (14), it is possible that other particle types could be more effective for *Bacillus anthracis* specific capture. A larger panel of magnetic particles should be tested to determine if the chemistry from an alternate affinity bait interacts in such a way with *B. anthracis* biomarkers to improve capture or stabilize them under these storage conditions. Additionally, steps could be taken to allow for the testing of the Nanotrap particles to stabilize proteins. Given the difficulties of using whole blood for western blot analysis we could alternatively incorporate wash

steps, to remove blood from Nanotrap particles. We could also potentially attempt to stabilize and enrich from serum as an alternative matrix.

Further studies should be conducted to identify which affinity bait is best suited for *B. anthracis*, as well as conducting protection assays to assess the particle's ability to stabilize analytes. This paper has shown magnetic CN3080 NT particles, functionalized with Reactive Red 120, are able to enrich bacterial and protein capture, bind and potentially stabilize nucleic acid. This ability to use magnetic NT particles to capture target analytes can allow for quick separation from complex biological matrices for easier workflow and downstream processing and possibly increased detection.

MATERIALS AND METHODS

Bacterial Strain, Human Whole Blood, and NT Particles

Bacillus anthracis, Sterne 34F2 (LLNL A0517), NR-1400 (BEI Resources, NIAID, NIH) was grown at 37°C in Luria Broth (LB) or on Luria Agar unless otherwise specified. Human whole blood, from a pooled, mixed gender sample suspended in K₂EDTA, was obtained from BioIVT (www.bioivt.com). Magnetic NTs were provided by Ceres Nanosciences, Inc., Manassas, VA (www.ceresnano.com). The NTs consisted of a cross-linked N-isopropylacrylamide (NIPAm) copolymerized with allylamine. These hydrogel particles were then functionalized with Reactive Red 120 and ferromagnetic fragments.

Bacterial Binding and Stability in Blood

B. anthracis Sterne colonies were resuspended in LB to 0.5 McFarland, and then diluted (1:20) in human whole blood. 200 µL of spiked blood was transferred to microcentrifuge tubes with (50 µL at 5 mg/mL) and without NTs. Samples were incubated at room temperature (RT) rotating 30 minutes for binding experiments, and at specified temperatures for the designated amount of time for stability experiments. Binding was determined by pelleting NT samples via magnetic rack (MagRack 6, GE Healthcare) for <1 minute, the supernatant removed and discarded. The remaining pellet

was then resuspended in 200 μ L LB. For stability experiments, the entire NT samples were processed without pelleting. Serial dilutions and plating on Luria agar were performed to determine CFU/mL.

Bacterial Enrichment

B. anthracis Sterne was grown at 37°C in Brain Heart Infusion (BHI) broth and diluted in Dulbecco's Phosphate Buffer Saline (DPBS) to 0.5 McFarland. The diluted culture was diluted to 1×10^3 CFU/mL in DPBS, transferring 1 mL mixture to microcentrifuge tubes in the absence or presence of traditional NTs or lyophilized NTs (5 mg/mL). Samples were incubated at RT, rotating for 2 hours. NT samples were pelleted and supernatant discarded. The pellet was resuspended in 100 μ L DPBS with 0.01% Tween-20. Serial dilutions and plating were performed to determine CFU/mL.

Comparison of Pelleting NTs to Centrifugation

B. anthracis Sterne was grown at 37°C in Brain Heart Infusion (BHI) broth and diluted in DPBS to 0.5 McFarland. The diluted culture was diluted to 1×10^4 CFU/mL in blood, transferring 1 mL mixture to microcentrifuge tubes in the absence or presence of lyophilized NTs (5 mg/mL). Samples were incubated at RT, rotating for 2 hours. The control samples were centrifuged at 6,000xg for 10 minutes, and NT samples pelleted on rack and supernatant discarded. Pellets for the control and NT samples were resuspended in 100 μ L DPBS with 0.01% Tween-20. Serial dilutions and plating were performed to determine CFU/mL.

Whole Cell Lysate

B. anthracis Sterne was grown at 37°C in Luria broth. Culture was centrifuged at 6000xg at 4°C for 10 minutes, the supernatant discarded. The pellet was resuspended in 50 mM Tris-HCl and then sonicated on ice at 40% amplitude (Q500 Sonicator, QSonica) in 30 second pulses until culture appeared clear. The lysate was then centrifuged at 15,000xg at 4°C for 10 minutes, the supernatant filtered using a 0.22 µM filter and stored at -80°C.

Preparation of NT-Bound Proteins for Proteomics Analysis

200 µL of undiluted whole cell lysate was transferred to microcentrifuges with and without NTs. For “Bacteria bound to NT” samples, *B. anthracis* Sterne was grown at 37°C in LB and diluted in DPBS to 0.5 McFarland. 200 µL of diluted culture was added to microcentrifuge tubes in the presence and absence of NTs. Samples were incubated at RT, rotating for 30 minutes. After incubation, NT samples were pelleted and supernatant discarded. Control and NT samples were submitted to Dr. Weidong Zhou for further processing. Samples were mixed with 8M Urea (20 µL) and incubated (50°C, 2 min). After incubation and centrifugation, the supernatant was reduced (10mM DTT), alkylated (50mM iodoacetamide), and digested with trypsin (37°C, 2 h). Post-digestion, samples were desalted (ZipTip), dried (SpeedVac), and then resuspended in 0.1% formic acid (10 µL).

LC-MS/MS Proteomic Analysis

Digested samples were analyzed on an Orbitrap Fusion (ThermoFisher Scientific, Waltham, MA, USA) equipped with a nanospray HPLC system (EASY-nLC 1200). Peptides were separated using a reversed-phase Acclaim PepMap RSLC C18 (2 μm , 75 μm i.d. \times 15 cm) column (ThermoFisher Scientific). After injection, the column was washed with mobile phase A (0.1% aqueous formic acid) and peptides were eluted using a linear gradient of 5% mobile phase B (0.1% formic acid in 80% acetonitrile) to 40% mobile phase B (60 min, 300 nL/min) and then to 100% mobile phase B (2 min).

The Orbitrap Fusion was operated in a data-dependent mode, where each full mass spectrometric scan (60,000 resolving power, 300 to 1500 Da) using quadrupole isolation was followed by MS/MS scans, in which the most abundant molecular ions were dynamically selected by Top Speed and fragmented by collision-induced dissociation (CID) (35% normalized collision energy). The peptide monoisotopic precursor selection, dynamic exclusion (10 s duration), and charge state dependency (+2 to +4) enabled.

Tandem mass spectra were searched against the *B. anthracis* Sterne NCBI database (Assembly GCA_000832635.1) with Proteome Discover (version 2.1). Mass tolerance for the precursor ion was set to 2 ppm and 0.5 Da for the fragment ion. Data was analyzed with variable modification for oxidation on methionine (M, +15.9949 Da) and fixed modification for carbamidomethylation on cysteine (C, +57.0215). Peptide spectrum matches (PSM) were reported with a cut-off value set to a 1% false discovery rate (FDR).

Analysis of Proteomic Data

Enrichment of proteins by NTs was calculated based on protein abundance (#PSMs). The values were first normalized, by taking the #PSMs for an individual protein and dividing it by the total #PSMs in a sample. Then, the enrichment values were calculated by taking the normalized value for NT-bound protein divided by normalized value for control protein. Enrichment had a >2.5-fold cutoff. Enriched proteins were also visualized for protein-protein interactions using String (<https://string-db.org>).

Proteins for control and experimental groups were also categorized based on subcellular-localization prediction using PSORTb (www.psort.org/psortb).

Western Blots

Bacillus anthracis Sterne whole cell lysate was diluted (1:10) in DPBS, human whole blood or diluted human whole blood (1:4 in DPBS), 200 μ L transferred to microcentrifuge tubes without and with NTs (5 mg/mL) and incubated (RT, 30 min). Post-incubation, NT samples were pelleted on magnetic rack and supernatant discarded. NT samples were resuspended in 30 μ L of 2x Laemmli Buffer (BioRad). Laemmli Buffer was added to control sample for a final 1x solution. Samples were heated in a water bath at 95°C for 5 minutes. NT samples were pelleted, and the eluent and control samples loaded onto a NuPAGE 4-12% gradient Bis-Tris gel, ran at 180V for 30 minutes. The gel was transferred to a PVDF membrane via a dry gel transfer system using an iBlot 2 transfer stack (7 min, 20V). The membrane was incubated in blocking buffer (5% nonfat

dry milk, in Tris Buffer Saline with 0.1% Tween 20 (TBS-T)) for one hour, before 4°C overnight incubation in primary polyclonal antibody to SodA-1, NR-10506 (BEI Resources, NIAID, NIH) (1:5000). Membrane was washed with TBS-T (3x, 5 min) and then incubated at RT in HRP-conjugated goat anti-rabbit secondary antibody (1:10000). Membrane was washed with TBS-T (3x, 5 min) and then incubated 5 minutes in West Femto Maximum Sensitivity Substrate (Pierce). Blot was visualized using Bio-Rad ChemiDoc imager.

DNA Extraction and qPCR

Nucleic acid was purified using DNeasy UltraClean Microbial Kit (Qiagen) with the following modifications: PowerBead Solution and 100 µL of Solution SL was added to the samples and then incubated on a heat block (70°C, 10 min) prior to transferring samples to PowerBead tubes. PCR reactions were set up using SYBR Green Perfecta Mastermix (Quantabio). Previously published primers to target the chromosomal element, PL3 (55), and the pXO1 plasmid gene (*pag*) which encodes for protective antigen (PA) (57) were purchased from Invitrogen. The following set of primers were used at a final 300nM concentration: PL3 forward primer 5'—AAA GCT ACA AAC TCT GAA ATT TGT AAA TTG—3' and PL3 reverse primer 5'—CAA CGA TGA TTG GAG ATA GAG TAT TCT TT—3', PA forward primers 5'—CGG ATC AAG TAT ATG GGA ATA TAG CAA—3' and PA reverse primer 5'—CCG GTT TAG TCG TTT CTA ATG GAT—3'. QPCR analysis was performed using thermocycler C1000 Touch with CFX96 Touch Real-Time PCR Detection System (Bio-Rad) under the following

conditions: 95°C for 5 mins, 40 cycles of 95°C for 15 sec and 58°C for 1 min with a plate read, and melt curve following end of entire run. PCR reactions were validated for specified target genes by loading samples onto 1.5% agarose gel with ethidium bromide and conducting gel electrophoresis. Bands were visualized using a Bio-Rad ChemiDoc imager.

Nucleic Acid Binding and Stability

Purified nucleic acid concentration was determined using the Nanodrop™ Lite Spectrophotometer (ThermoFisher). Human whole blood was spiked with 20 ng of nucleic acid per sample, and 200 µL transferred to microcentrifuge tubes without and with NTs (5 mg/mL). Samples were incubated rotating for 30 minutes at RT to assess NT binding ability and at 54°C up to 72 h to assess stability. When testing for binding, NT samples were pelleted on MagRack and blood removed, pellet was resuspended in DPBS as a wash step, pelleted again and supernatant discarded. The resulting pellet was resuspended in PowerBead and SL solution and processed as outlined for DNA extraction. For stability experiments, DPBS (100-200 µL) was added to the blood post-incubation to allow for easier processing at the later time points (24-72 h), the entire samples (+NT, -NT) being purified.

DNase Protection Assay

Human whole blood was spiked with 20 ng of purified nucleic acid and incubated in the presence or absence of NTs (37°C, 30 min. After initial incubation, 25 µL of 10X Reaction Buffer and 50 µL (1 U/ µL) DNase I, RNase-free (ThermoScientific) was added

to the samples to be challenged with DNase. The samples were then incubated at 37°C overnight, approximately 20 hours. Post-incubation 25 µL EDTA was added to all samples, including those without DNase, and incubated on a heat block at 65°C for 10 minutes to stop further degradation. NT samples were pelleted using the MagRack and supernatant discarded, washed once with PBS and then resuspended in PowerBead and SL solution. After resuspension, all samples were processed for nucleic acid and qPCR as previously described.

Bacteria to Nucleic Acid Experiment

B. anthracis Sterne colonies were resuspended in LB to 3 McFarland, diluted (1:100) in DPBS and then diluted again 1:20 in blood. 200 µL of spiked blood was transferred to microcentrifuge tubes with (50 µL at 5 mg/mL) and without NTs. Samples were incubated at 54°C up to 72 h. Post-incubation, The NT samples were pelleted, supernatant discarded, followed by a PBS wash, and resulting pellet resuspended in PowerBead and SL solution as previously described.

Software and Statistical Analysis

Graphs and statistical analysis were conducted using GraphPad Prism software (version 8) for Mac OS (GraphPad Software, San Diego, CA). Student's *t*-test were performed unless otherwise noted, with p-value < 0.05 considered to be significant.

REFERENCES

1. WHO. 2008. Anthrax in humans and animals. World Health Organization.
2. Liu D. 2014. Manual of Security Sensitive Microbes and Toxins, 1st ed doi:<https://doi.org/10.1201/b16752>. CRC press.
3. Carlson CJ, Getz WM, Kausrud KL, Cizauskas CA, Blackburn JK, Bustos Carrillo FA, Colwell R, Easterday WR, Ganz HH, Kamath PL, Okstad OA, Turner WC, Kolsto AB, Stenseth NC. 2018. Spores and soil from six sides: interdisciplinarity and the environmental biology of anthrax (*Bacillus anthracis*). *Biol Rev Camb Philos Soc* 93:1813-1831.
4. Roth NG, Lively DH, Hodge HM. 1955. Influence of Oxygen Uptake and Age of Culture of Sporulation of *Bacillus Anthracis* and *Bacillus Globigii*. *J Bacteriol* 69:455-459.
5. Moayeri M, Leppia SH, Vrentas C, Pomerantsev AP, Liu S. 2015. Anthrax Pathogenesis. *Annu Rev Microbiol* 69:185-208.
6. ASM. 2017. Sentinel Level Clinical Laboratory Guidelines for Suspected Agents of Bioterrorism and Emerging Infectious Diseases: *Bacillus anthracis* and *Bacillus cereus* biovar *anthracis*. American Society for Microbiology.
7. Sedlackova V, Dziedzinska R, Babak V, Kralik P. 2017. The detection and quantification of *Bacillus thuringiensis* spores from soil and swabs using quantitative PCR as a model system for routine diagnostics of *Bacillus anthracis*. *J Appl Microbiol* doi:10.1111/jam.13445.
8. Bentahir M, Ambroise J, Delcorps C, Pilo P, Gala JL. 2018. Sensitive and Specific Recombinase Polymerase Amplification Assays for Fast Screening, Detection, and Identification of *Bacillus anthracis* in a Field Setting. *Appl Environ Microbiol* 84.
9. Luchini A, Geho DH, Bishop B, Tran D, Xia C, Dufour RL, Jones CD, Espina V, Patanarut A, Zhou W, Ross MM, Tessitore A, Petricoin EF, 3rd, Liotta LA. 2008. Smart hydrogel particles: biomarker harvesting: one-step affinity purification, size exclusion, and protection against degradation. *Nano Lett* 8:350-61.
10. Shafagati N, Patanarut A, Luchini A, Lundberg L, Bailey C, Petricoin E, 3rd, Liotta L, Narayanan A, Lepene B, KeHN-Hall K. 2014. The use of Nanotrap particles for biodefense and emerging infectious disease diagnostics. *Pathog Dis* 71:164-76.
11. Kim B, Araujo R, Howard M, Magni R, Liotta LA, Luchini A. 2018. Affinity enrichment for mass spectrometry: improving the yield of low abundance biomarkers. *Expert Rev Proteomics* 15:353-366.

12. Capriotti AL, Caruso G, Cavaliere C, Piovesana S, Samperi R, Lagana A. 2012. Comparison of three different enrichment strategies for serum low molecular weight protein identification using shotgun proteomics approach. *Anal Chim Acta* 740:58-65.
13. Shafagati N, Lundberg L, Baer A, Patanarut A, Fite K, Lepene B, Kehn-Hall K. 2015. The use of Nanotrap particles in the enhanced detection of Rift Valley fever virus nucleoprotein. *PLoS One* 10:e0128215.
14. Akhrymuk I, Lin SC, Sun M, Patnaik A, Lehman C, Altamura L, Minogue T, Lepene B, van Hoek ML, Kehn-Hall K. 2020. Magnetic Nanotrap Particles Preserve the Stability of Venezuelan Equine Encephalitis Virus in Blood for Laboratory Detection. *Front Vet Sci* 6:509.
15. Fredolini C, Meani F, Reeder KA, Rucker S, Patanarut A, Botterell PJ, Bishop B, Longo C, Espina V, Petricoin EF, 3rd, Liotta LA, Luchini A. 2008. Concentration and Preservation of Very Low Abundance Biomarkers in Urine, such as Human Growth Hormone (hGH), by Cibacron Blue F3G-A Loaded Hydrogel Particles. *Nano Res* 1:502-518.
16. Lin SC, Carey BD, Callahan V, Lee JH, Bracci N, Patnaik A, Smith AK, Narayanan A, Lepene B, Kehn-Hall K. 2020. Use of Nanotrap particles for the capture and enrichment of Zika, chikungunya and dengue viruses in urine. *PLoS One* 15:e0227058.
17. Rasko DA, Worsham PL, Abshire TG, Stanley ST, Bannan JD, Wilson MR, Langham RJ, Decker RS, Jiang L, Read TD, Phillippy AM, Salzberg SL, Pop M, Van Ert MN, Kenefic LJ, Keim PS, Fraser-Liggett CM, Ravel J. 2011. *Bacillus anthracis* comparative genome analysis in support of the Amerithrax investigation. *Proc Natl Acad Sci U S A* 108:5027-32.
18. Wattam AR, Davis JJ, Assaf R, Boisvert S, Brettin T, Bun C, Conrad N, Dietrich EM, Disz T, Gabbard JL, Gerdes S, Henry CS, Kenyon RW, Machi D, Mao C, Nordberg EK, Olsen GJ, Murphy-Olson DE, Olson R, Overbeek R, Parrello B, Pusch GD, Shukla M, Vonstein V, Warren A, Xia F, Yoo H, Stevens RL. 2017. Improvements to PATRIC, the all-bacterial Bioinformatics Database and Analysis Resource Center. *Nucleic Acids Res* 45:D535-D542.
19. Chung MC, Tonry JH, Narayanan A, Manes NP, Mackie RS, Gutting B, Mukherjee DV, Popova TG, Kashanchi F, Bailey CL, Popov SG. 2011. *Bacillus anthracis* interacts with plasmin(ogen) to evade C3b-dependent innate immunity. *PLoS One* 6:e18119.
20. Witzky A, Tollerson R, 2nd, Ibbas M. 2019. Translational control of antibiotic resistance. *Open Biol* 9:190051.
21. Aharonowitz Y, Ron EZ. 1976. Translocation in *Bacillus subtilis*: Characterization of Elongation Factor G by Peptidyl-[3H]puromycin Synthesis. *J Bacteriol*:1074-1079.
22. Rosenberg A, Soufi B, Ravikumar V, Soares NC, Krug K, Smith Y, Macek B, Ben-Yehuda S. 2015. Phosphoproteome dynamics mediate revival of bacterial spores. *BMC Biol* 13:76.

23. Volker U, Engelmann S, Maul B, Riethdorf S, Volker A, Schmid R, Mach H, Hecker M. 1994. Analysis of the induction of general stress proteins of *Bacillus subtilis*. *Microbiology* 140:741-752.
24. Mayer MP, Bukau B. 2005. Hsp70 chaperones: cellular functions and molecular mechanism. *Cell Mol Life Sci* 62:670-84.
25. Shi L, Ravikumar V, Derouiche A, Macek B, Mijakovic I. 2016. Tyrosine 601 of *Bacillus subtilis* DnaK Undergoes Phosphorylation and Is Crucial for Chaperone Activity and Heat Shock Survival. *Front Microbiol* 7:533.
26. Chitlaru T, Gat O, Gozlan Y, Ariel N, Shafferman A. 2006. Differential proteomic analysis of the *Bacillus anthracis* secretome: distinct plasmid and chromosome CO₂-dependent cross talk mechanisms modulate extracellular proteolytic activities. *J Bacteriol* 188:3551-71.
27. Antelmann H, Williams RC, Miethke M, Wipat A, Albrecht D, Harwood CR, Hecker M. 2005. The extracellular and cytoplasmic proteomes of the non-virulent *Bacillus anthracis* strain UM23C1-2. *Proteomics* 5:3684-95.
28. Adekambi T, Drancourt M, Raoult D. 2009. The *rpoB* gene as a tool for clinical microbiologists. *Trends Microbiol* 17:37-45.
29. Maughan H, Galeano B, Nicholson WL. 2004. Novel *rpoB* mutations conferring rifampin resistance on *Bacillus subtilis*: global effects on growth, competence, sporulation, and germination. *J Bacteriol* 186:2481-6.
30. Nicholson WL, Maughan H. 2002. The spectrum of spontaneous rifampin resistance mutations in the *rpoB* gene of *Bacillus subtilis* 168 spores differs from that of vegetative cells and resembles that of *Mycobacterium tuberculosis*. *J Bacteriol* 184:4936-40.
31. Brown JR, Gentry D, Becker JA, Ingraham K, Holmes DJ, Stanhope MJ. 2003. Horizontal transfer of drug-resistant aminoacyl-transfer-RNA synthetases of anthrax and Gram-positive pathogens. *EMBO Rep* 4:692-8.
32. Lincecum Jr. T, Tukalo M, Yaremchuk A, Mursinna R, Williams A, Sproat B, Van Den Eynde W, Link A, Van Calenbergh S, Grotli M, Martinis S, Cusack S. 2003. Structural and Mechanistic Basis of Pre- and Posttransfer Editing by Leucyl-tRNA Synthetase. *Mol Cell* 11:951-963.
33. Kermgard E, Yang Z, Michel AM, Simari R, Wong J, Ibba M, Lazizzera BA. 2017. Quality Control by Isoleucyl-tRNA Synthetase of *Bacillus subtilis* Is Required for Efficient Sporulation. *Sci Rep* 7:41763.
34. Kochetov GA, Solovjeva ON. 2014. Structure and functioning mechanism of transketolase. *Biochim Biophys Acta* 1844:1608-18.
35. Fraenkel D, Vinopal R. 1973. CARBOHYDRATE METABOLISM IN BACTERIA. *Annu Rev Microbiol* 27:69-100.
36. Walz A, Mujer CV, Connolly JP, Alefantis T, Chafin R, Dake C, Whittington J, Kumar SP, Khan AS, DeVecchio VG. 2007. *Bacillus anthracis* secretome time course under host-simulated conditions and identification of immunogenic proteins. *Proteome Sci* 5:11.
37. Salje J, van den Ent F, de Boer P, Lowe J. 2011. Direct membrane binding by bacterial actin MreB. *Mol Cell* 43:478-87.

38. Defeu Soufo HJ, Graumann PL. 2005. *Bacillus subtilis* actin-like protein MreB influences the positioning of the replication machinery and requires membrane proteins MreC/D and other actin-like proteins for proper localization. *BMC Cell Biol* 6:10.
39. Strahl H, Burmann F, Hamoen LW. 2014. The actin homologue MreB organizes the bacterial cell membrane. *Nat Commun* 5:3442.
40. Cybulski RJ, Jr., Sanz P, Alem F, Stibitz S, Bull RL, O'Brien AD. 2009. Four superoxide dismutases contribute to *Bacillus anthracis* virulence and provide spores with redundant protection from oxidative stress. *Infect Immun* 77:274-85.
41. Lee JY, Passalacqua KD, Hanna PC, Sherman DH. 2011. Regulation of petrobactin and bacillibactin biosynthesis in *Bacillus anthracis* under iron and oxygen variation. *PLoS One* 6:e20777.
42. Tu WY, Pohl S, Gray J, Robinson NJ, Harwood CR, Waldron KJ. 2012. Cellular iron distribution in *Bacillus anthracis*. *J Bacteriol* 194:932-40.
43. Szklarczyk D, Gable AL, Lyon D, Junge A, Wyder S, Huerta-Cepas J, Simonovic M, Doncheva NT, Morris JH, Bork P, Jensen LJ, Mering CV. 2019. STRING v11: protein-protein association networks with increased coverage, supporting functional discovery in genome-wide experimental datasets. *Nucleic Acids Res* 47:D607-D613.
44. Sparacino-Watkins C, Stolz JF, Basu P. 2014. Nitrate and periplasmic nitrate reductases. *Chem Soc Rev* 43:676-706.
45. Tiso M, Schechter AN. 2015. Nitrate reduction to nitrite, nitric oxide and ammonia by gut bacteria under physiological conditions. *PLoS One* 10:e0119712.
46. Gusarov I, Shatalin K, Starodubtseva M, Nudler E. 2009. Endogenous Nitric Oxide Protects Bacteria Against a Wide Spectrum of Antibiotics. *Science* 325:1380-1384.
47. Shatalin K, Gusarov I, Avetissova E, Shatalina Y, McQuade LE, Lippard SJ, Nudler E. 2008. *Bacillus anthracis*-derived nitric oxide is essential for pathogen virulence and survival in macrophages. *Proc Natl Acad Sci U S A* 105:1009-13.
48. Kiran M, Bala S, Hirshberg M, Balaban N. 2010. YhgC protects *Bacillus anthracis* from oxidative stress. *Int J Artif Organs* 33:590-607.
49. Fedhila S, Msadek T, Nel P, Lereclus D. 2002. Distinct clpP genes control specific adaptive responses in *Bacillus thuringiensis*. *J Bacteriol* 184:5554-62.
50. McGillivray SM, Ebrahimi CM, Fisher N, Sabet M, Zhang DX, Chen Y, Haste NM, Aroian RV, Gallo RL, Guiney DG, Friedlander AM, Koehler TM, Nizet V. 2009. ClpX contributes to innate defense peptide resistance and virulence phenotypes of *Bacillus anthracis*. *J Innate Immun* 1:494-506.
51. Gerth U, Kruger E, Derre I, Msadek T, Hecker M. 1998. Stress induction of the *Bacillus subtilis* clpP gene encoding a homologue of the proteolytic component of the Clp protease and the involvement of ClpP and ClpX in stress tolerance. *Mol Microbiol* 28:787-802.
52. Chitlaru T, Ariel N, Zvi A, Lion M, Velan B, Shafferman A, Elhanany E. 2004. Identification of chromosomally encoded membranal polypeptides of *Bacillus*

- anthracis by a proteomic analysis: prevalence of proteins containing S-layer homology domains. *Proteomics* 4:677-91.
53. Missiakas D, Schneidwind O. 2017. Assembly and Function of the *Bacillus anthracis* S-Layer. *Annu Rev Microbiol* 71:79-98.
 54. Agren J, Hamidjaja RA, Hansen T, Ruuls R, Thierry S, Vigre H, Janse I, Sundstrom A, Segerman B, Koene M, Lofstrom C, Van Rotterdam B, Derzelle S. 2013. In silico and in vitro evaluation of PCR-based assays for the detection of *Bacillus anthracis* chromosomal signature sequences. *Virulence* 4:671-85.
 55. Wielinga PR, Hamidjaja RA, Agren J, Knutsson R, Segerman B, Fricker M, Ehling-Schulz M, de Groot A, Burton J, Brooks T, Janse I, van Rotterdam B. 2011. A multiplex real-time PCR for identifying and differentiating *B. anthracis* virulent types. *Int J Food Microbiol* 145 Suppl 1:S137-44.
 56. Marston CK, Gee JE, Popovic T, Hoffmaster AR. 2006. Molecular approaches to identify and differentiate *Bacillus anthracis* from phenotypically similar *Bacillus* species isolates. *BMC Microbiol* 6:22.
 57. Ellerbrok H, Nattermann H, Ozel M, Beutin L, Appel B, Pauli G. 2002. Rapid and sensitive identification of pathogenic and apathogenic *Bacillus anthracis* by real-time PCR. *FEMS Microbiology Letters* 214:51-59.
 58. Cieslik P, Knap J, Kolodziej M, Mirski T, Joniec J, Graniak G, Zakowska D, Winnicka I, Bielawska-Drozd A. 2015. Real-Time PCR Identification of Unique *Bacillus anthracis* Sequences *Folia Biological (Praha)* 61:178-183.

BIOGRAPHY

Brittany Heath graduated from Marion Senior High School, Marion, Virginia, in 2008. She received her Bachelor of Science from Virginia Polytechnic Institute and State University (Virginia Tech) in 2012 and a second Bachelor of Science from Virginia Tech in 2015. In 2017, she pursued a Masters in Biology at George Mason University with a concentration in Microbiology and Infectious Diseases.